

## Removal of Norfloxacin Antibiotic from Aqueous Solution by Activated Carbon Prepared from Pomelo Peel Biomass Waste by Chemical Activation

Panida Prarat<sup>1\*</sup>, Kamolchanok Hadsakunnee<sup>2</sup>,  
Lucksamee Padejapan<sup>2</sup>, Kanyaruk Prasertboonyai<sup>1</sup>

<sup>1</sup>*Faculty of Science, Energy and Environment, King Mongkut's University of Technology North Bangkok (Rayong Campus), Rayong 21220, Thailand*

<sup>2</sup>*Department of Agro-Industrial, Food and Environmental Technology, Faculty of Applied Science, King Mongkut's University of Technology North Bangkok, Bangkok 10800, Thailand*

\*Corresponding : panida.p@sciee.kmutnb.ac.th

---

### Abstract

As Biomass waste, pomelo peel was used as precursor for activated carbon (ACs) preparation by phosphoric acid (PPA) and diammonium hydrogen orthophosphate (DAP) activation and to examine the feasibility of removing norfloxacin antibiotic (NOR) from aqueous solution. Characterizations of the ACs were performed using N<sub>2</sub> adsorption-desorption isotherms, Fourier-transform infrared spectroscopy (FT-IR), Elemental Analysis (EA), and Acid base titration. The BET analysis showed that PPA activation (P-PPA) possesses a higher porosity than DAP activation (P-DAP) with BET surface area of 626.92 m<sup>2</sup>/g. P-DAP shows a wealth of nitrogen-containing functional groups. Batch adsorption experiments indicated that NOR was adsorbed onto the P-DAP higher than P-PPA. The kinetic data of the adsorption process followed the pseudo-second order model, and the equilibrium data were described well by Freundlich isotherm. NOR adsorption was found to be strongly dependent on the pH of solution as well as the pK<sub>a</sub> of both adsorbents and NOR. The strong adsorptive interaction between NOR and adsorbents was mainly attributed to the combination interactions i.e. electrostatic interaction, hydrogen bonding and hydrophobic interactions. Moreover, the presence of ions on adsorption process significantly decreased the NOR adsorption onto P-DAP due to the competitive adsorption.

**Keywords:** Adsorption, Activated carbon, Norfloxacin removal, Chemical activation

---

### 1. Introduction

Emerging micropollutants such as pharmaceutical compounds, hormones, personal care products, and antibiotic compounds are one of the major concerns in the production of drinking water and release of wastewater to the environment (Rossner *et al.*, 2009). Fluoroquinolone antibiotic are a group of

synthetic chemicals, extensively used in human and veterinary medicine and agriculture. It has been detected in the various fates such as wastewater, surface water, production plants, manufacturing and hospital with a wide range of concentrations (0.2 ppb- 30 ppm). Even in low concentrations, the persistence of antibiotics could lead to the development of antibiotic-resistant bacteria and has been suggested as

an environmental micro-pollutant hazard. Therefore, the effective removal of antibiotic as the micropollutants has become an increasingly important issue (Halling-Sørensen *et al.*, 2000).

Fluoroquinolones are among the five class of antibiotics (fluoroquinolones, macrolides, sulfonamides, and tetracyclines) frequently detected at relatively high concentrations in the environment (Khetan & Collins, 2007). Residues of them discharged from agricultural runoff and municipal wastewater treatment plants are frequently detected in surface water, groundwater, and drinking water (Sun *et al.*, 2010). The widespread of fluoroquinolones has become a serious problem as it has a variety of potential adverse effects, including acute and chronic toxicity. Because fluoroquinolones antibiotics have been shown to disrupt microbial respiration and be poorly metabolized, the removal of fluoroquinolones antibiotics by conventional water and wastewater treatment technologies is generally incomplete (Jia *et al.*, 2012).

Adsorption is a well-known effective technique for pollutants removal because of its easy operation, insensitivity to toxic substances, and the possibility of reusing the spent adsorbent (Niu *et al.*, 2013). Activated carbons are promising materials for a variety of potential applications due to their well-developed porosity and rich surface functional groups. However, in recent years, the industrial production of activated carbon is facing the problem of raw material scarcity and high cost, with the result that its price is getting higher and higher, so as to limit it to be widely used in the treatment of pollutants. So, it has become hot spot of current research to seek cheap raw material to lower preparation cost of activated carbon. Several suitable agricultural waste/by-products i.e., olive-wastecakes (Baccar *et al.*, 2009), including cattle-manure compost (Zaini *et al.*, 2009), bamboo materials (Lo *et al.*, 2012), potato peel (Moreno-Piraján & Giraldo, 2011), have been investigated in the last years as activated carbon precursors and are still receiving renewed attention. Recently, Sun *et al.* use pomelo peel as precursors for activated carbons preparation by phosphoric

acid activation and found that it exhibited larger surface area and portion of mesoporous (Sun *et al.*, 2016). The mesoporous structure is expected to be excellent pharmaceutical residue removal from aqueous solution.

The adsorption capacity of porous carbon depends on not only its surface area and pore structure, but also functional groups on its pore surface. The functional groups and pore structure of porous carbon commonly determine its application. As a result, chemical and physical modifications occur on the surfaces of activated carbons. The surface chemistry may be modified by various techniques, such as acid treatment, ammonization, and microwave treatment (Wenzhong *et al.*, 2008). The activation methods for preparing activated carbon mainly include physical and chemical activation. With regard to physical activation, the usual commercial choices of activation gas are CO<sub>2</sub> and steam. And, the usual activation agent for chemical activation are H<sub>3</sub>PO<sub>4</sub>, KOH, NaOH, K<sub>2</sub>CO<sub>3</sub>, ZnCl<sub>2</sub> and so forth.

The previous study by Benaddi *et al.* used di-ammonium hydrogen orthophosphate ((NH<sub>4</sub>)<sub>2</sub>HPO<sub>4</sub>) as activation agent to prepare activated carbon from wood, indicated that activated carbon had comparable properties of phosphoric acid (H<sub>3</sub>PO<sub>4</sub>), and the carbon structure was predominantly microporous (Benaddi *et al.*, 2000). Moreover, the amino functional group, as well as hydroxyl functional groups, play a significant role in the field of antibiotic adsorption. Nevertheless, there was rare work to prepare activated carbon using (NH<sub>4</sub>)<sub>2</sub>HPO<sub>4</sub> from agricultural wastes. The aim of this study, di-ammonium hydrogen orthophosphate was selected as the activation agent. Waste pomelo peel was selected as precursor material to prepare activated carbon by chemical activation method and test them as adsorbents for norfloxacin (NOR) removal from aqueous solution. Activated carbon prepared by phosphoric acid chemical activation was studied for comparison. Of course there are work regarding the use of pomelo peel for adsorption application (Sun *et al.*, 2016), but none with NOR as removal pollutant. The objective of the research was to (1) investigate the effects

of the process parameters on NOR adsorption; (2) discuss the adsorption mechanism between NOR and activated carbon based on the isotherm models; and (3) evaluate the influence of coexisting ions on NOR adsorption onto carbon adsorbents.

## 2. Materials and Methods

### 2.1 Materials

All the primary chemicals used in this study were of analytical grade. Distilled water was utilized throughout the experiments for solution preparation and glassware cleaning. Norfloxacin ( $C_{16}H_{18}FN_3O_3$ ) from Sigma-Aldrich was used as adsorbate. With  $pK_{a1} = 6.22$  and  $pK_{a2} = 8.51$  for the carboxylic acid and the basic-N-moiety group, the speciation of cation (NOR<sup>+</sup>), zwitterion (NOR<sup>+/-</sup>) and anion (NOR<sup>-</sup>) were existed under different pH. Di-ammonium hydrogen orthophosphate ((NH<sub>4</sub>)<sub>2</sub>HPO<sub>4</sub>); DAP, and phosphoric acid (85 %wt); PPA, were provided from Ajax Finechem and QREC, respectively.

### 2.2 Preparation of activated carbon

Activated carbon were prepared using following simple method. Pomelo peel used for preparation of activated carbon was obtained locally. The precursor was first washed with distilled water, dried, cut, and sieved to desired mesh size of 1–2 mm. After immersing in DAP or PPA solution at a ratio of 1:3 (g precursor/g activate reagents), the wet sample was soaked for 24 h. Then, the samples were washed distilled water until the pH was neutral and dried at 105 °C for 24 h. Then, the samples were with heated at temperature of 800 °C and was hold at the carbonization temperature for 1 h. Finally, the carbon was ground, sieved and kept in desiccator until use. The produced carbon adsorbent is designated P-DAP and P-PPA, respectively.

### 2.3 Characterization of adsorbents

The physiochemical characteristics of synthesized adsorbents were characterized by several techniques. N<sub>2</sub> adsorption-desorption isotherms were analyzed with an V-Sorb

2800P surface area and pore volume analyzer (Gold APP Instruments, China) at 77 °K. X-ray powder diffraction (XRD) patterns were obtained on a Bruker AXS D8 diffractometer using Cu-K $\alpha$  radiation. The adsorbents were determined the pH at the point of zero charge (pHPZC) by the acid-base titration method (Peng *et al.*, 2014). Fourier transform infrared (FT-IR) spectrophotometry was recorded on a Perkin Elmer Spectrum One using KBr pellets to analyze the presence of surface functional group and interaction between adsorbent and antibiotic. Elemental analysis was carried out using a LECO Coporation, 628 Series.

### 2.4 Adsorption experiments

Batch adsorption experiment was studies in 125-ml Erlenmeyer flask containing 0.57 g/L of carbon adsorbent. The solution pH and ionic strength was controlled by using a 0.01 M phosphate buffer. NOR stock was prepared in methanol at 1000 mg/L. The experimental sample was conducted with shaking condition at 200 rpm (30 °C), and then filtered through a glass filter (GF/C, pore size 0.45  $\mu$ m). The quantities of NOR concentration in equilibrium solutions were analyzed by a UV-Vis spectrophotometer at 270 nm. The NOR uptake at the equilibrium  $q_e$  (mg/g) was calculated as follows:

$$q_e = \frac{(C_0 - C_e)V}{m} \quad (1)$$

where  $C_0$  and  $C_e$  (mg/L) are the initial and equilibrium concentrations of NOR, respectively;  $V$ (L) is the volume of the solution; and  $m$  (g) is the dosage of the adsorbent.

Adsorption kinetic, the experiment was performed by varying the contact time and initial NOR concentration at 25 mg/L in 0.01 M phosphate buffer pH 7.0. According to adsorption isotherm, the experiment was performed as described in the adsorption kinetic study except the concentration of NOR varied between 5 mg/L and 50 mg/L. While the effect of the pH on the adsorption capacity was investigated at pH 5, pH 7 and pH 9.

All the experimental samples were performed in duplicate, and the average values are reported. Additional analyses were

conducted whenever two measurements showed a difference larger than 5%.

### 2.5 Data analysis

The kinetics of the adsorption process were determined using the pseudo-first-order and pseudo-second-order rate adsorption kinetic models, as indicated in the Equation (2) and (3), respectively as follows:

$$\log(q_e - q_t) = \log q_e - \frac{k_1}{2.303} t \quad (2)$$

$$\frac{t}{qt} = \frac{1}{k_2(q_e^2)} + \frac{t}{q_e} \quad (3)$$

where  $q_e$  and  $q_t$  (mg/g) are the NOR adsorption capacities and adsorbed at equilibrium and  $t$  (min), respectively.  $k_1$  is the pseudo-first-order rate constant (1/min), and  $k_2$  is the rate constant of pseudo-second order adsorption (g/mg.min).

Langmuir and Freundlich isotherm models were investigated the sorption process in this work. In generally, Langmuir equation can be described the monolayer adsorption process and the homogeneous adsorptive surface. Whereas Freundlich equation is used for the multilayer adsorption process and the heterogeneous adsorptive surface. The Langmuir and Freundlich equation can be represented by the Equation (4) and (5), respectively as follows:

Langmuir isotherm

$$\frac{1}{q_e} = \frac{1}{K_L q_m} \cdot \frac{1}{C_e} + \frac{1}{q_m} \quad (4)$$

Freundlich isotherm

$$\ln q_e = \frac{1}{n} \ln C_e + \ln K_F \quad (5)$$

where  $q_m$  (mg/g) is the theoretical maximum adsorption capacity,  $K_L$  (L/mg) is the Langmuir isotherm constant,  $C_e$  is NOR equilibrium concentration (mg/L),  $K_F$ (L/mg) and  $n$  are Freundlich isotherm constant and heterogeneity factor indicating the adsorption intensity of the adsorbent, respectively.

## 3. Results and Discussion

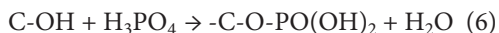
### 3.1 Adsorbent Characterization

The  $N_2$  adsorption/desorption isotherms is an important parameter for the adsorption of organic pollutants in aqueous solution. Fig. 1 showed the  $N_2$  adsorption/desorption isotherms and pore size distributions of P-DAP and P-PPA, respectively. According to the results, the isotherm of P-PPA and P-DAP, the isotherms are mixture of type I and type IV with hysteresis loops (Figure. 1a), indicating the co-existence of micropores and mesopores. The BET specific surface area, total pore volume and mesopore size of the samples are shown in Table 1.

The porous structural parameters are shown in Table 1. The BET surface area of P-PPA (626.92  $m^2/g$ ) is higher than that of P-DAP (83.79  $m^2/g$ ). P-PPA has total pore volume of 0.35  $cm^3/g$ , microporous volume of 0.07  $cm^3/g$ , and mesoporous volume of 0.28  $cm^3/g$ , while P-DAP has total pore volume of 0.08  $cm^3/g$ , microporous volume of 0.02  $cm^3/g$ , and mesoporous volume of 0.06  $cm^3/g$ . The mean pore size of P-PPA and P-DAP is 2.23 and 4.03 nm, respectively. It is reported that the precursor has a great effect on the pore size distribution of activated carbon. Figure. 1b shows that P-PPA and P-DAP has a larger portion of mesoporous located in 20 nm. These pores are advantage for large size molecular adsorption.

FT-IR spectroscopy (Figure. 2) was used to identify the major functional groups of the adsorbent. In Fig. 2, the band at around 3400-3500  $cm^{-1}$  can be assigned to the O-H stretching vibration of the hydroxyl functional groups, due to the existence of cellulose and lignin (Liang et al., 2011). The peak located around 2930  $cm^{-1}$  corresponds to C-H stretching (Zhang et al., 2017) in methyl and methylene groups. The band around 1650-1662  $cm^{-1}$  is attributed to an aromatic carbon or carboxyl groups, respectively (stretch of C-C in aromatic rings or stretch of C-O). The bands at 1385  $cm^{-1}$  could be ascribed to phenolic C-O and O-H stretching modes. A small peak at 1034  $cm^{-1}$  could result from ionized linkage  $P+O^-$  in acid phosphates and to symmetrical vibration in a

chain of C-O-P as Equation (6) (Liu *et al.*, 2012)



Elemental compositions (C, H, O and N) of the adsorbent are presented in Table 2. As can be seen, the content of N of P-DAP was larger than that of P-PPA. The two types of carbon have obvious difference in elemental composition, suggesting that they have significantly different surface functional groups. It can also be seen in Fig. 3 the results of surface charge. The point of zero charge ( $\text{pH}_{\text{PZC}}$ ) of P-DAP and P-PPA are 4.30-5.09 and 6.28, respectively. The increase in the  $\text{pHPZC}$  values of P-DAP compared with P-PPA which can be explained due to by nitrogen-incorporation rendered the carbon surface more basic after ammonia tailoring, thus creating a surface that was more positively charged, resulted in increasing of the  $\text{pHPZC}$  values.

### 3.2 Adsorption kinetic

Figure. 4 shows the time profile of adsorption of NOR from aqueous solution

onto P-DAP and P-PPA. The kinetic profiles all show an initial rapid uptake step (<30 min) followed by a slower, incremental uptake step with equilibrium reached within 4 and 8 hr. for P-DAP and P-PPA, respectively. The P-DAP has better uptake efficiency and removal capacity for NOR in comparison with the P-PPA. This can be explained that the increase in surface basicity may partly be a consequence of the formation of basic surface functionalities that are capable of binding with fluoroquinolone antibiotics (Liu *et al.*, 2011).

The kinetic parameters and correlation coefficients of the kinetics models are shown in Table 3. The correlation coefficients of the pseudo-second-order kinetic model are higher than pseudo-first-order. That is to say, the adsorption process for NOR onto two carbons adsorbents can be well described by the pseudo-second-order kinetic equation. This result also exhibited that different adsorption mechanisms are involved in the adsorption process including chemical and physical adsorption, while the physical adsorption dominated in the adsorption process (Jung *et al.*, 2013).

**Table 1.** Structural properties of adsorbents.

| Adsorbents | $S_{\text{REY}}$<br>( $\text{m}^2/\text{g}$ ) | $D_p$<br>(nm) | $V_{\text{total}}$<br>( $\text{cm}^3/\text{g}$ ) | $V_{\text{mic}}$<br>( $\text{cm}^3/\text{g}$ ) | $V_{\text{mes}}$<br>( $\text{cm}^3/\text{g}$ ) |
|------------|---|---------------|--|--|--|
| P-DAP      | 83.79   | 4.03          | 0.08   | 0.02   | 0.06   |
| P-PPA      | 626.92  | 2.23          | 0.35   | 0.07   | 0.28   |

\* The average pore diameter.

**Table 2.** Elemental analysis of the various adsorbents.

| Adsorbents | C<br>(wt%) | H<br>(wt%) | N<br>(wt%) | O and other<br>(wt%) |
|------------|------------|------------|------------|----------------------|
| P-DAP      | 53.62      | 2.82       | 2.07       | 41.49                |
| P-PPA      | 60.08      | 3.45       | 0.93       | 35.54                |

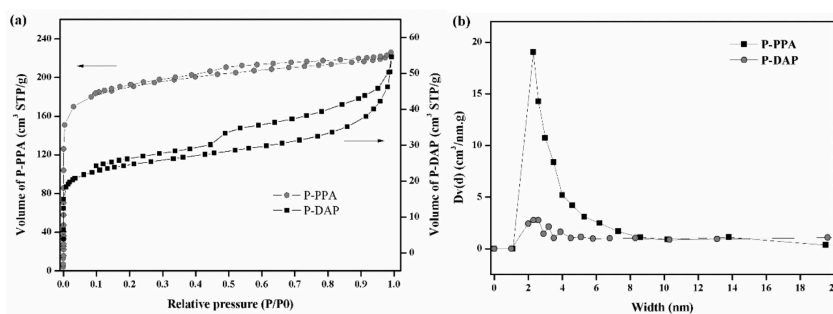


**Figure 1.** Nitrogen adsorption/desorption isotherms and pore size distribution of P-DAP and P-PPA adsorbents.

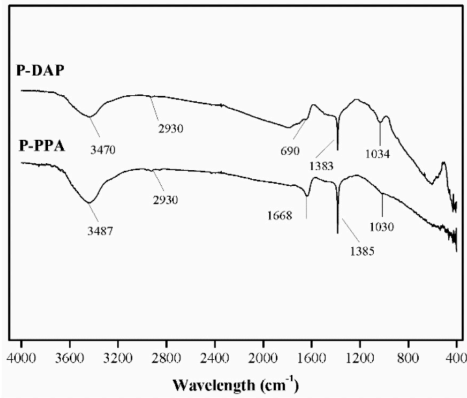


Figure 2. The FT-IR of adsorbents.

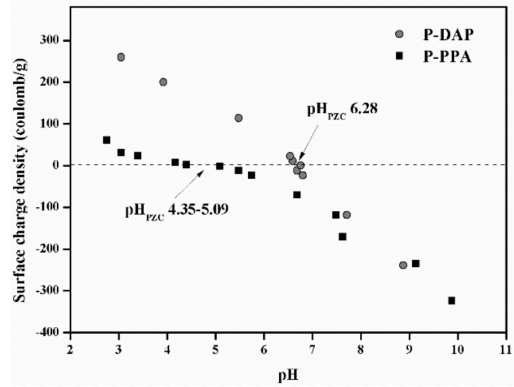


Figure 3. Surface charge density of adsorbents at various pH of solution.

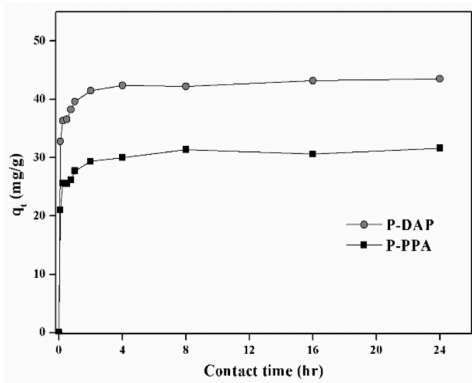


Figure 4. Adsorption kinetic of NOR onto P-DAP and P-PPA

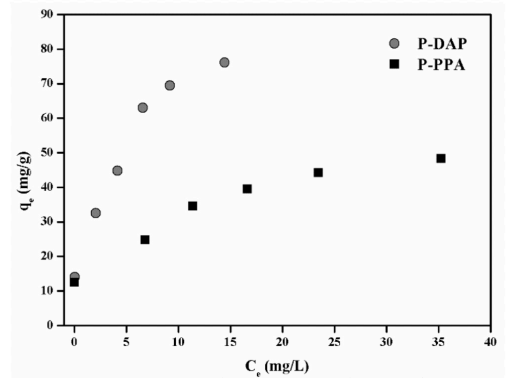


Figure 5. Adsorption isotherm of NOR onto P-DAP and P-PPA.

Table 3. Kinetic parameters of NOR onto P-DAP and P-PPA.

| Adsorbents | $q_{e,exp}$ | Pseudo-first order model                  |       |                                  |
|------------|-------------|---|-------|----------------------------------|
|            |             | $K_1$<br>( $\text{min}^{-1}$ )            | $R^2$ | $q_{e,cal}$<br>( $\text{mg/g}$ ) |
| P-DAP      | 45.39       | 0.05                                      | 0.68  | 9.55                             |
| P-PPA      | 34.23       | 0.05                                      | 0.75  | 9.74                             |
| Adsorbents | $q_{e,exp}$ | Pseudo-second order model                 |       |                                  |
|            |             | $K_2$<br>( $\text{g/mg}\cdot\text{min}$ ) | $R^2$ | $q_{e,cal}$<br>( $\text{mg/g}$ ) |
| P-DAP      | 45.39       | 0.07                                      | 0.99  | 48.08                            |
| P-PPA      | 34.23       | 0.06                                      | 0.99  | 36.90                            |

Table 4 Isotherm parameters of NOR onto P-DAP and P-PPA.

| Adsorbent | Langmuir                   |                            |       |
|-----------|----------------------------|----------------------------|-------|
|           | $q_m$<br>( $\text{mg/g}$ ) | $K_L$<br>( $\text{L/mg}$ ) | $R^2$ |
| P-DAP     | 101.35                     | 0.223                      | 0.996 |
| P-PPA     | 38.34                      | 29.65                      | 0.906 |
| Adsorbent | Freundlich                 |                            |       |
|           | $K_F$<br>( $\text{L/mg}$ ) | $1/n$                      | $R^2$ |
| P-DAP     | 33.98                      | 0.275                      | 0.997 |
| P-PPA     | 23.67                      | 0.168                      | 0.978 |

### 3.3 Adsorption isotherms

To further understand the adsorption mechanism of NOR onto the two carbon materials. Langmuir and Freundlich adsorption models were used to fit the experimental data. The adsorption model parameters were listed in Table 4. From the table can be seen, both the Langmuir and the Freundlich models fitted the NOR isotherm well on the P-DAP, however, the exponent  $1/n$  value for P-DAP was fairly less than half in the Freundlich models, which means that the form of the NOR adsorption equilibrium on P-DAP was more Freundlich like than Langmuir model. In case of P-PPA, the Freundlich model fits the experiment data better than Langmuir model by comparing the determination coefficients. Thus, these results indicate that the adsorption behavior of the two carbons is characterized by the heterogeneous adsorptive surface. In addition, the presence of nitrogen-containing functional groups on the surface of adsorbent enhanced the adsorption of NOR.

It is evident from Table 1 that P-DAP and P-PPA are predominated by mesopores. The P-PPA has higher surface area and larger total volume in comparison with the P-DAP. Surprisingly, P-DAP exhibit much better sorption and stronger adsorption affinity to NOR (Fig. 5), even though the lower surface area and total volume compared to P-PPA. It can be ascribed to the more basic P-DAP is more favored adsorption NOR due to the dispersive interactions between the delocalized electrons in the P-DAP carbon materials basal planes and the free electrons (aromatic rings) in the NOR molecule.

### 3.4 Effect of pH on NOR adsorption capacity

Batch adsorption experiment was conducted at solution pH of 5, 7 and 9 and P-DAP was chosen for studying due to higher was chosen for studying due to higher adsorption capacity than that of P-PPA. Generally, a NOR molecule consists of a bicyclic aromatic ring skeleton with a carboxylic acid group ( $pK_{a1} \sim 6.22$ ), a ketone group, and a basic-N-moiety ( $pK_{a2} \sim 8.51$ ). However, the existing NOR species, a cation (NOR<sup>+</sup>),

zwitterion (NOR<sup>±</sup>), and anion (NOR<sup>-</sup>), depend on the pH of the solution, therefore, each NOR speciation's persistence is considered (NOR species was shown in Fig. 6).

As mentioned above, the pH of the solution affects the ionizable functional group of NOR molecular structure, therefore, the adsorption interaction can be affected due to change in pH. Not only the speciation of NOR can change with the pH but also the surface functional groups on P-DAP. However, all of this experimental condition (a pH range of solution between pH 5-9), the surface charge of P-DAP illustrated as the cationic, closely neutral charge and negative charge at pH 5, pH 7 and pH 9, respectively as shown in Fig. 3. According to the adsorption of NOR onto P-DAP, it can be seen that The adsorption process was low pH (pH 5) and the adsorption capacity of P-DAP increased with the elevate pH value, which can reach the maximum values of 76.12 mg/g under the tested concentration was observed at pH 7. The surface of all the adsorbents is positively charged at pH lower than pHPZC and negatively charged at pH higher than pHPZC. At solution  $pH < pK_{a1}$  ( $pK_{a1} = 6.22$ ), the NOR molecules and adsorbents surface have opposite charges, thus adsorption is expected to be enhanced. When  $pH > pK_{a2}$  ( $pK_{a2} = 8.51$ ), the anionic form of NOR is the dominant species in the aqueous solutions. In this stage, the amounts of NORP adsorbed onto four adsorbents are expected to be depressed, because NOR molecules and adsorbents surfaces were negatively charged and can repel each other (Carabineiro *et al.*, 2011). These are consistent with the experimental data. Therefore, electrostatic interaction between NOR and P-DAP played the key role influencing the adsorption process. Beside electrostatic interaction, the hydrogen bonding and hydrophobic reaction are another mechanism for the adsorption of NOR molecules.

### 3.5 Effect of coexisting ions on NOR adsorption

Figure 8 shows the effect of four cation electrolytes on the adsorption of NOR on P-DAP. Changing the ionic concentration from 0 mM to 100 mM has mixed effects on NOR adsorption on P-DAP. It was observed

that the presence of  $\text{Na}^+$  slightly inhibited adsorption of NOR on the P-DAP since 60 mM of  $\text{Na}^+$  concentration. However,  $\text{Mg}^{2+}$ ,  $\text{NO}_3^-$  and  $\text{SO}_4^{2-}$  had a much greater inhibiting effect on adsorption capacities. This might be due to the different interaction mechanisms between ions and adsorbent. Ions inhibit the adsorption of NOR by competing for surface sites, reducing the electrostatic attraction between NOR and P-DAP. Comparing between monovalent and divalent ion effect, the replacing power of ion increases with its charge (Figuroa *et al.*, 2004), which may explain why  $\text{Mg}^{2+}$ , and  $\text{SO}_4^{2-}$  inhibited adsorption more than  $\text{Na}^+$  and  $\text{NO}_3^-$ .

### 5. Conclusions

Activated carbon derived from biomass by diammonium hydrogen orthophosphate (DAP) and phosphoric acid (P-PPA) activation exhibited a high ratio of mesopore structure

(>70%). P-DAP possessed much less surface area in comparison with P-PPA. For adsorption isotherm, P-DAP contained much more amino surface functional groups and exhibited much higher NOR adsorption capacities than P-PPA. The electrostatic interaction, hydrogen bonding and hydrophobic reaction played the key role influencing the NOR adsorption process. The presence of cationic and anionic ions impeded the NOR adsorption due to the competitive adsorption.

### 6. Acknowledgements

This research was funded by King Mongkut's University of Technology North Bangkok; Contract no. KMUTNB-62-KNOW-33. Moreover, we would like to thank Faculty of Science, Energy and Environment, King Mongkut's University of Technology North Bangkok (KMUTNB) for the equipment.

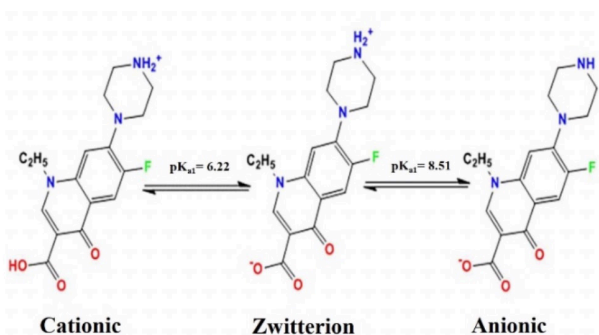


Figure 6. the speciation of NOR in aqueous solution as a function of the solution pH.

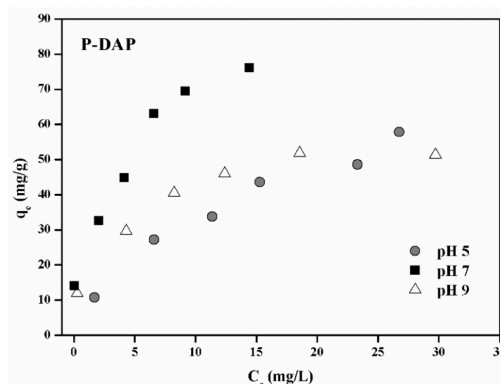


Figure 7. Effect of pH on adsorption of NOR onto P-DAP

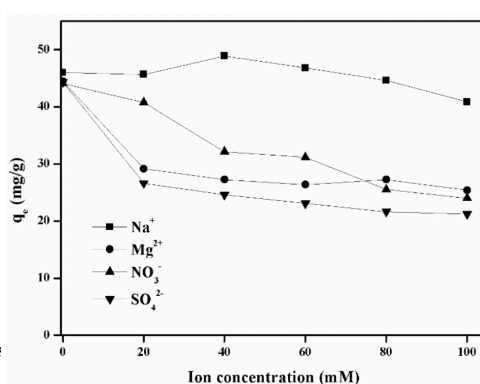


Figure 8. Influence of ions on NOR adsorption onto p-DAP at pH 7.



## 7. References

- Baccar, R., Bouzid, J., Feki, M., Montiel, A. 2009. Preparation of activated carbon from Tunisian olive-waste cakes and its application for adsorption of heavy metal ions. *Journal of Hazardous Materials*, 162, 1522-1529.
- Benaddi, H., Bandosz, T.J., Jagiello, J., Schwarz, J.A., Rouzaud, J.N., Legras, D., Béguin, F. 2000. Surface functionality and porosity of activated carbons obtained from chemical activation of wood. *Carbon*, 38, 669-674.
- Carabineiro, S.A.C., Thavorn-Amornsri, T., Pereira, M.F.R., Figueiredo, J.L. 2011. Adsorption of ciprofloxacin on surface-modified carbon materials. *Water Research*, 45(15), 4583-4591.
- Figuroa, R.A., Leonard, A., MacKay, A.A. 2004. Modeling Tetracycline Antibiotic Sorption to Clays. *Environmental Science & Technology*, 38, 476-483.
- Halling-Sørensen, B., Holten Lützhøft, H.-C., Andersen, H.R., Ingerslev, F. 2000. Environmental risk assessment of antibiotics: comparison of mecillinam, trimethoprim and ciprofloxacin. *Journal of Antimicrobial Chemotherapy*, 46, 53-58.
- Jia, A., Wan, Y., Xiao, Y., Hu, J. 2012. Occurrence and fate of quinolone and fluoroquinolone antibiotics in a municipal sewage treatment plant. *Water Research*, 46, 387-394.
- Jung, C., Heo, J., Han, J., Her, N., Lee, S.-J., Oh, J., Ryu, J., Yoon, Y. 2013. Hexavalent chromium removal by various adsorbents: Powdered activated carbon, chitosan, and single/multi-walled carbon nanotubes. *Separation and Purification Technology*, 106, 63-71.
- Khetan, S.K., Collins, T.J. 2007. Human Pharmaceuticals in the Aquatic Environment: A Challenge to Green Chemistry. *Chemical Reviews*, 107, 2319-2364.
- Liang, S., Guo, X., Tian, Q. 2011. Adsorption of  $Pb^{2+}$  and  $Zn^{2+}$  from aqueous solutions by sulfured orange peel. *Desalination*, 275, 212-216.
- Liu, H., Zhang, J., Bao, N., Cheng, C., Ren, L., Zhang, C. 2012. Textural properties and surface chemistry of lotus stalk-derived activated carbons prepared using different phosphorus oxyacids: Adsorption of trimethoprim. *Journal of Hazardous Materials*, 235-236, 367-375.
- Liu, W., Zhang, J., Zhang, C., Ren, L. 2011. Sorption of norfloxacin by lotus stalk-based activated carbon and iron-doped activated alumina: Mechanisms, isotherms and kinetics. *Chemical Engineering Journal*, 171, 431-438.
- Lo, S.-F., Wang, S.-Y., Tsai, M.-J., Lin, L.-D. 2012. Adsorption capacity and removal efficiency of heavy metal ions by Moso and Ma bamboo activated carbons. *Chemical Engineering Research and Design*, 90, 1397-1406.
- Moreno-Piraján, J.C., Giraldo, L. 2011. Activated carbon obtained by pyrolysis of potato peel for the removal of heavy metal copper (II) from aqueous solutions. *Journal of Analytical and Applied Pyrolysis*, 90, 42-47.
- Niu, Y., Qu, R., Sun, C., Wang, C., Chen, H., Ji, C., Zhang, Y., Shao, X., Bu, F. 2013. Adsorption of  $Pb(II)$  from aqueous solution by silica-gel supported hyperbranched polyamidoamine dendrimers. *Journal of Hazardous Materials*, 244-245, 276-286.
- Peng, X., Hu, X., Fu, D., Lam, F.L.Y. 2014. Adsorption removal of acid black 1 from aqueous solution using ordered mesoporous carbon. *Applied Surface Science*, 294, 71-80.
- Rossner, A., Snyder, S.A., Knappe, D.R.U. 2009. Removal of emerging contaminants of concern by alternative adsorbents. *Water Research*, 43, 3787-3796.
- Sun, H., Shi, X., Mao, J., Zhu, D. 2010. Tetracycline sorption to coal and soil humic acids: An examination of humic structural heterogeneity. *Environmental Toxicology and Chemistry*, 29, 1934-1942.

- Sun, Y., Li, H., Li, G., Gao, B., Yue, Q., Li, X. 2016. Characterization and ciprofloxacin adsorption properties of activated carbons prepared from biomass wastes by H<sub>3</sub>PO<sub>4</sub> activation. *Bioresource Technology*, 217, 239-244.
- Wenzhong, S., Zhijie, L., Yihong, L. 2008. Surface Chemical Functional Groups Modification of Porous Carbon. *Recent Patents on Chemical Engineering (Discontinued)*, 1, 27-40.
- Zaini, M.A.A., Okayama, R., Machida, M. 2009. Adsorption of aqueous metal ions on cattle-manure-compost based activated carbons. *Journal of Hazardous Materials*, 170, 1119-1124.
- Zhang, X., Niu, J., Zhang, X., Xiao, R., Lu, M., Cai, Z. 2017. Graphene oxide-SiO<sub>2</sub> nanocomposite as the adsorbent for extraction and preconcentration of plant hormones for HPLC analysis. *Journal of Chromatography B*, 1046, 58-64.